Supporting Information

Used abbreviations for ionic liquids

[BMIM] 1-butyl-3-methyl-imidazolium
[EMIM] 1-ethyl-3-methyl-imidazolium
[PYR13] N-methyl-N-propylpyrrolidinium
[BF_4] tetrafluoroborate
[TFSI] bis(trifluoromethylsulfonyl)imide

Used abbreviations for thermophysical properties

T_g glass transition temperature
T_m melting temperature
T_f freezing temperature

Table S1: Table of physical properties of selected ionic liquids

	Density (g/cm^3)	**Conductivity (mS/cm) at 293-298 K**	**Viscosity (mPa·s)**	**Melting point (K)**	**Freezing point (K)**	**Reference**
[EMIM][BF_4]	1.24-1.28	11.6-15.8	37-66	284-288	210-222	S1
[BMIM][BF_4]	1.21	2.3-3.5	180	186	-	S2
[PYR13][TFSI]	1.45	3.2-3.6	63	279-285	-	S2

Materials characterization

Transmission electron microscopy (TEM) samples were prepared by dispersing powders in ethanol and placing the solution over a copper grid with a lacey carbon film. Measurements on BP2000 were carried out on a JEOL 2100F operating at 200 kV.

Raman spectra were recorded with a Renishaw inVia Raman Microscope using an Nb-YAG laser with an excitation wavelength of 532 nm and a grating with 1800 lines/mm yielding a spectral resolution of ~1.2 cm^{-1}. The spot size on the sample was in the focal plane circa 2 µm using an output power of 0.5 mW. Spectra were recorded for 30 s and accumulated 50-times to eliminate cosmic rays and to obtain a high signal-to-noise and signal-to-background ratio.

To remove adsorbed molecules from the surface, all samples were degassed initially at 200 °C for 30 min and subsequently at 300 °C for 20 h at a relative pressure of 0.1 Pa. Nitrogen gas sorption analysis at 77 K was then performed with Quantachrome Autosorb iQ system. Using the Brauner-Emmett-Teller (BET) equation,[S3] the BET specific surface area (SSA) was calculated using a partial pressure range between 0.05 and 0.30 P/P_0 where a linear correlation with a positive *C*-constant and high R^2-value were obtained.[S4] The pore size distribution (PSD) was derived using the quenched-solid density functional theory (QSDFT)[S5-6] supplied by Quantachrome and a slit shape was assumed. For comparison, we also applied a mixed slit pore / cylindrical pore geometry (hybrid slit-cylindrical equilibrium kernel). The latter model assumes cylindrical pores from 2.12 to 50.2 nm and slit pores from 0.375 to 2.0 nm.[S5] Given the pressure range starting at $P/P_0 = 10^{-6}$, a smallest pore size of 0.57 nm could be resolved for the PSD.

Structure and porosity of porous carbons

BP2000 is a high surface area carbon black provided by Cabot Corporation. The particle size, determined by transmission electron microscopy (TEM), ranged between 20 and 50 nm (**Fig. S1A**) and, consistent with TEM (inset in **Fig. S1A**), Raman spectroscopy evidences the highly graphitic nature of the carbon black (**Fig. S1B**) by the presence of a predominant G-band peak at 1594 cm^{-1} and a small D-band peak at 1334 cm^{-1}.

The specific surface area was 1374 m^2/g using nitrogen gas sorption at -196 °C and BET analysis[S3] in the pressure range between 0.01 and 0.12 P/P_0 (following the recommendations of ISO/DIS9277).[S4] The isotherm shows a characteristic low-pressure range typical for microporous carbons (type I isotherm) and the high-pressure range is indicative of a predominance of mesopores (type IV isotherm).[40] Using quenched-solid density functional theory[S5-6] and assuming slit-shaped pores, the pore size distribution shows pores ranges from small micropores (<1 nm) to large mesopores (> 20 nm). The type H4-like hysteresis is indicative of slit-shaped pores.[S7] In combination, the total pore volume of meso- and micropores was 2 cm^3/g with 23 vol% micropores.

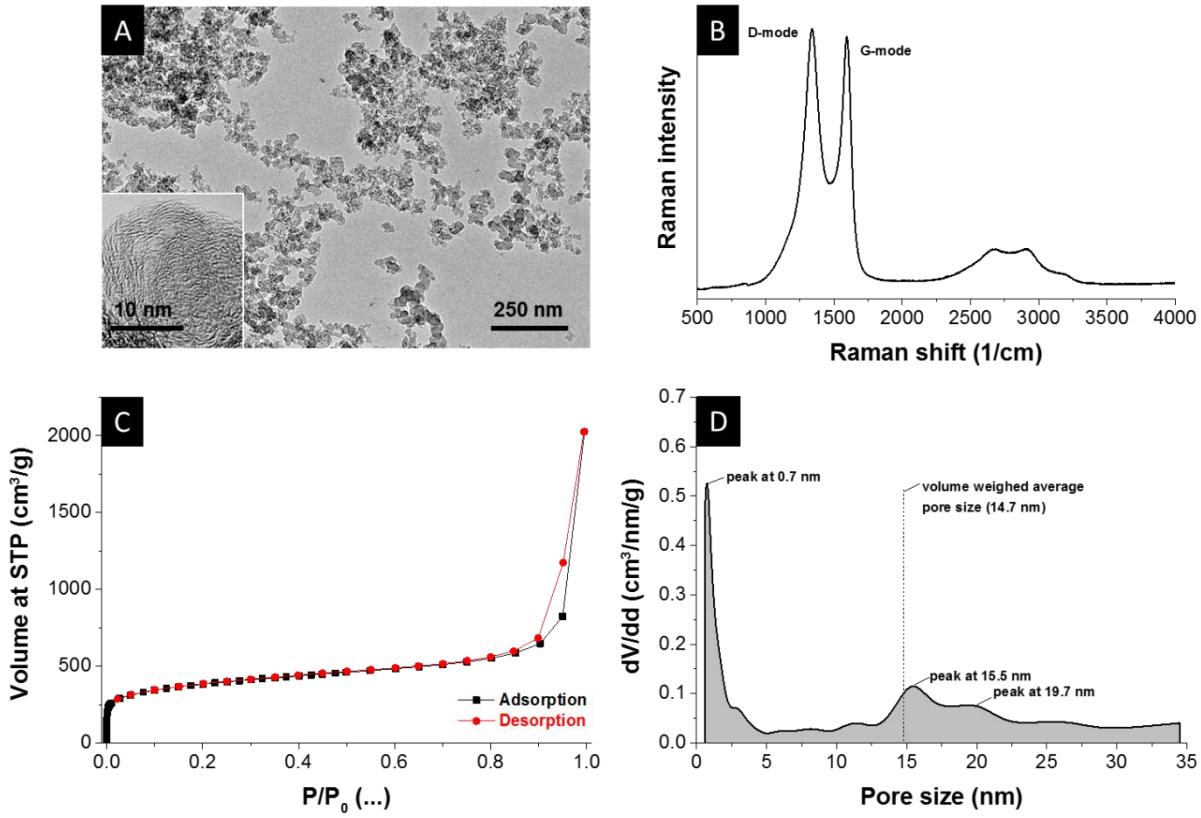

Figure S1. Characterization of BP2000, a high surface area nanoporous carbon black. TEM images (A), Raman spectrum (B), gas sorption isotherm (C), and differential pore size distribution (D).

Thermograms of [EMIM][BF_4] with different vertex temperatures

During the DSC measurements it turned out that the crystallization behavior of [EMIM][BF_4] is dependent on the upper vertex temperature before the system is cooled down. The corresponding thermograms are shown in **Fig. S2**. Going to an upper vertex temperature of +120 °C leads to a pronounced supercooling of the liquid and an exothermal signal upon heating. Going up to a temperature of +80 °C leads only to a partial exothermic peak during cooling while in the corresponding heating cycle from -80 °C the system showed again a broad exothermic peak at about -50 °C. Going to +60 °C leads to a larger exothermic peak during freezing which was still a bit smeared out towards lower temperatures, whereas an upper vertex temperature of +40 °C lead to a sharp crystallization peak at -40 °C. In addition the melting was influenced by the two freezing steps during cooling and heating, resulting in an additional small endothermic peak during heating of the system at about -5 °C, which clearly can be attributed to the exothermic peak during heating. It is completely absent in the thermogram only going to +40 °C.

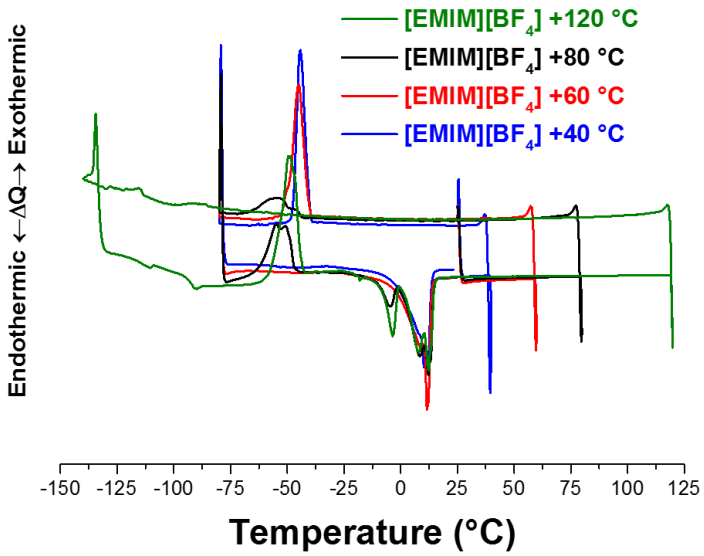

Figure S2. Thermograms of [EMIM][BF_4] in nanoconfinement up to different upper vertex temperatures. Scan rate: 10 °C/min.

Thermogram of 10 wt,% [BMIM][BF_4] in [EMIM][BF_4]

The thermogram of 10 wt,% [BMIM][BF_4] in [EMIM][BF_4] confined in nanoporous carbon is displayed in Figure S3. The crystallization takes place in two subsequent steps, partly during cooling and partly during the reheating of the sample, comparable to the thermogram of [EMIM][BF_4] with an upper vertex potential of +80 °C. However, even though the thermogram was only conducted up to 40 °C the peaks are much broader as compared to the bare [EMIM][BF_4] system.

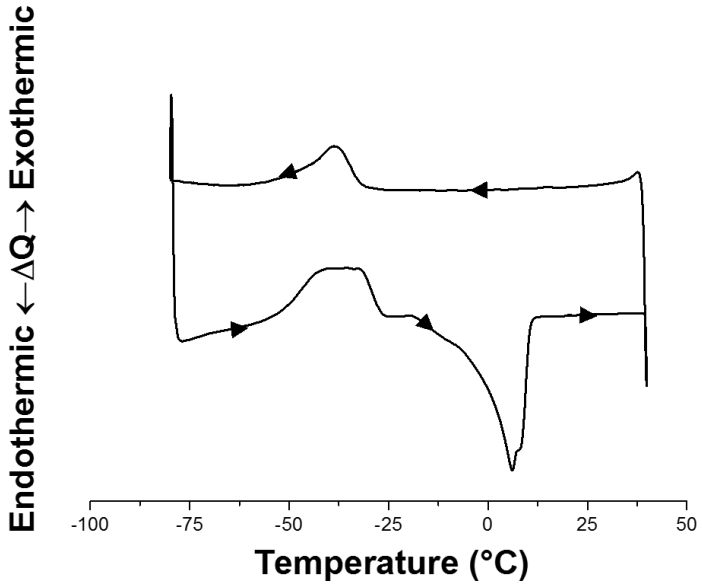

Figure S3. 10 wt,% [BMIM][BF_4] in [EMIM][BF_4] confined in a nanoporous carbon electrode. Scan rate: 10 °C/min.

Electrochemical charging and determination of the electrode potentials

The charged high surface area carbon electrodes for the DSC measurements with the respective electrolyte were achieved by charging a symmetric supercapacitor cell that contained a reference electrode to monitor the respective electrode potentials. These are reported in **Fig. S4** for the two investigated electrolytes. Due to slight mass imbalances and a probable imbalance of different capacitance for positive and negative electrode, the electrode potentials are slightly different for a charging of the cells to 2.5 V. For [PYR13][TFSI] the positive electrode stayed at +1.2 V vs. AC whereas the negative electrode reached -1.3 V vs. AC. For [EMIM][BF_4] the positive electrode reached 1.1 V vs. AC and the negative stayed at -1.4 V vs. AC.

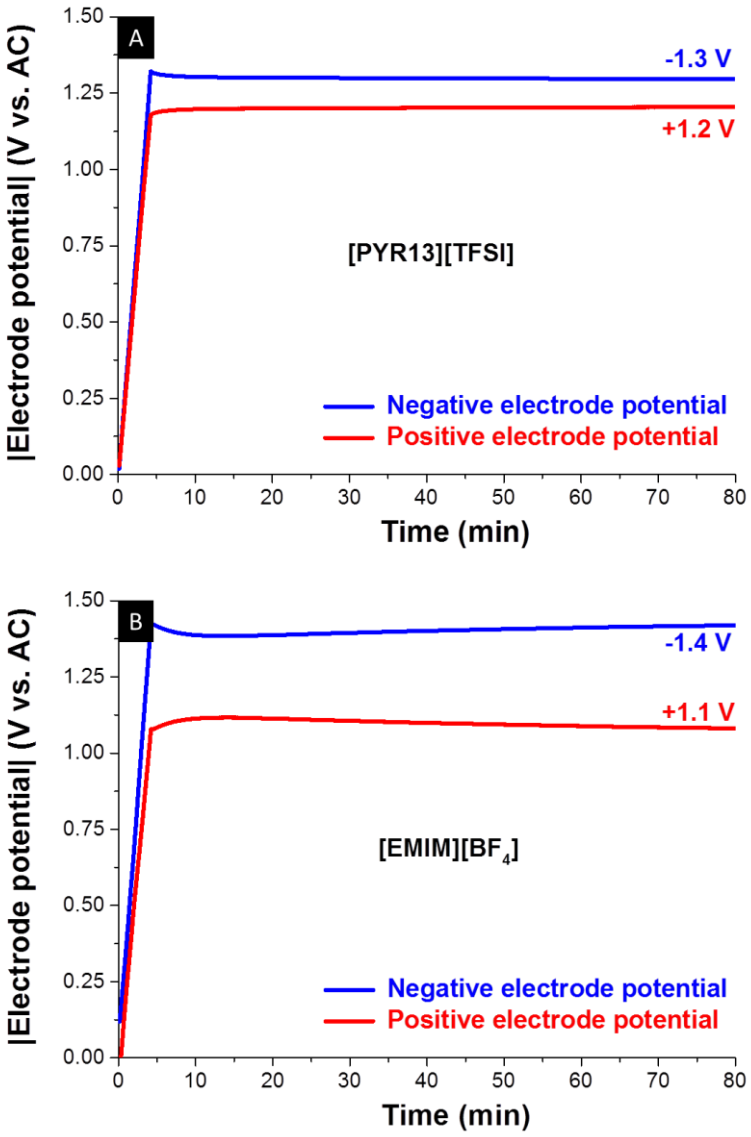

Figure S4. Time versus electrode potential for the ex situ DSC samples.

References

S1 Zhang, J.; Zhang, Q.; Li, X.; Liu, S.; Ma, Y.; Shi, F.; Deng, Y. Nanocomposites of ionic liquids confined in mesoporous silica gels: preparation, characterization and performance. Physical Chemistry Chemical Physics 2010, 12 (8), 1971-1981.

S2 MacFarlane, D. R.; Meakin, P.; Sun, J.; Amini, N.; Forsyth, M. Pyrrolidinium Imides: A New Family of Molten Salts and Conductive Plastic Crystal Phases. The Journal of Physical Chemistry B 1999, 103 (20), 4164-4170.

S3 Brunauer, S.; Emmett, P. H.; Teller, E. Adsorption of Gases in Multimolecular Layers. Journal of the American Chemical Society 1938, 60 (2), 309 - 319.

S4 BSI British Standards. Determination of the specific surface area of solids by gas adsorption - BET method. ISO/DIS 9277. 2008; Vol. ISO/DIS 9277.

S5 Gor, G. Y.; Thommes, M.; Cychosz, K. A.; Neimark, A. V. Quenched solid density functional theory method for characterization of mesoporous carbons by nitrogen adsorption. Carbon 2012, 50 (4), 1583-1590.

S6 Neimark, A. V.; Lin, Y.; Ravikovitch, P. I.; Thommes, M. Quenched solid density functional theory and pore size analysis of micro-mesoporous carbons. Carbon 2009, 47 (7), 1617 - 1628.

S7 Sing, K. S. W.; Everett, D. H.; Haul, R. A. V.; L. Moscou; Pierotti, R. A.; Rouquerol, J.; Siemieniewska, T. Reporting physisorption data for gas/solid systems with special reference to the determination of surface area and porosity (Recommendations 1984). Pure Appl Chem 1985, 57 (4), 603 - 619.